Variant selection criterion for twin variants in titanium alloys deformed by rolling

S Wang, C Schuman, L Bao, J.S. Lecomte, Y Zhang, J M Raulot, M J Philippe, X Zhao, C Esling

Variant Selection Criterion for Twin Variants in Titanium alloys deformed by rolling**.

By Shiying Wang, Christophe Schuman*, Lei Bao, Jean Sébastien Lecomte, Yudong Zhang, Jean Marc Raulot, Marie Jeanne Philippe, X. Zhao, Claude Esling

* Dr. C. Schuman
Laboratoire d'Étude des Microstructures et de Mécanique des Matériaux, LEM3, CNRS 7239, Université Paul Verlaine – Metz, Ile du Saulcy, 57045 Metz, France
E-mail : christophe.schuman@univ-metz.fr

S. Wang, Dr. L. Bao, J.S. Lecomte, Y. Zhang, J.M. Raulot, Prof. M.J. Philippe, C. Esling
LEM3, CNRS 7239, Université Paul Verlaine – Metz, Ile du Saulcy, 57045 Metz, France
X. Zhao
Key Laboratory for Anisotropy and Texture of Materials (Ministry of Education), Northeastern University, Shenyang 110819, People's Republic of China

A new selection criterion to explain the activation of the twinning variant is proposed based on the calculation of the deformation energy to create a primary twin. The calculation takes into account the effect of the grain size using a Hall-Petch type relation. This criterion allows to obtain a very good prediction for the variant selection. The calculations are compared with the experimental results obtained on T40 deformed by Rolling.

Introduction

Deformation twinning is one of the main deformation modes in crystalline solids particularly in low symmetry or multiple lattice structures [1-8]. Though extensive studies have addressed on the crystallography [9-11], morphology [12] and mechanical behavior [2, 13] of deformation twins, and numerous models for twinning have been suggested over the last few decades [14, 15], some fundamental issues remain unclear. The nucleation and growth mechanism of twin lamellae, the interaction of twinning with crystal defects, and the interfacial accommodation between the matrix and twins [16, 17] are still poorly understood.

In the case of titanium alloys, many authors have attempted to determine the presence of the different types of twins as a function of the deformation temperature or grain size [18, 19, 24] as well as to extract useful information for modeling [1, 20].

Although the twin type and the twin volume fraction can be easily determined [21], the type of variants present as well as the sequence in which they appear in one grain are not well revealed.

Recently, we have developed the "interrupted in situ SEM/EBSD orientation examination method" to follow the microstructure and crystallographic orientation evolution during the mechanical deformation process. This method allows us to obtain the time resolved information of the appearance of the twin variants, their growth, the interaction between them and the interaction with the initial grain boundaries [22]. However, the variant selection rules and the physical mechanisms behind still remain uncovered.

For magnesium and magnesium alloys that are also hexagonal materials but with different c/a ratio from that of titanium [17], Martin [24], Jonas [25] have proposed variant selection rules (Schmid Factor (SF), common volume) for the secondary twinning during deformation. Their criteria worked well for the deformed magnesium where the twins are thin. However, for titanium, it seems that the selection of the variants follows a different rule and should be clarified.

In the present work, we experimentally investigated the deformation process of commercially pure titanium with interrupted in situ SEM/EBSD orientation measurements. Based on the experimental examination, we tried to work out the twin variant selection rule. This rule is not established by a mere statistical examination to have statistical representation but to reveal the physical and mechanical criteria (energy) of variant selection that would useful for the modeling of the mechanical behavior of the alloys.

Material and Sample preparation

The material was hot-rolled and then annealed commercial pure titanium sheet of 1.5 mm thickness with the composition given in table 1.

Table 1 Chemical composition of commercially pure titanium T40

Element	H	C	N	O	Fe	Ti
Composition (ppm(wt.))	3	52	41	1062	237	Balance

A grain growth annealing was performed at 750°C for 30 minutes to produce a recrystallized microstructure. After annealing, the samples were mechanically ground up to 4000 #-grit SiC paper and then electrolytically polished at 5°C and 17V for 30 seconds in a solution of 10 ml perchloric acid in 90 ml methanol.

The samples were rolled in one step with 10% reduction. To follow the deformation of the individual grains during the deformation, a 500×300 μm^2 area was carefully polished and marked out with four micro-indentations. The orientation of all the grains in this polished area (about 800 grains) was measured by SEM/EBSD before and after each deformation step. Fig. 1 is the sketch of the rolling. Before rolling, the two sample plates as shown in Fig. 1 were firmly stuck together to avoid sliding during the compression in order to maintain a good surface quality [22]. This technique is also known as split sample technique.

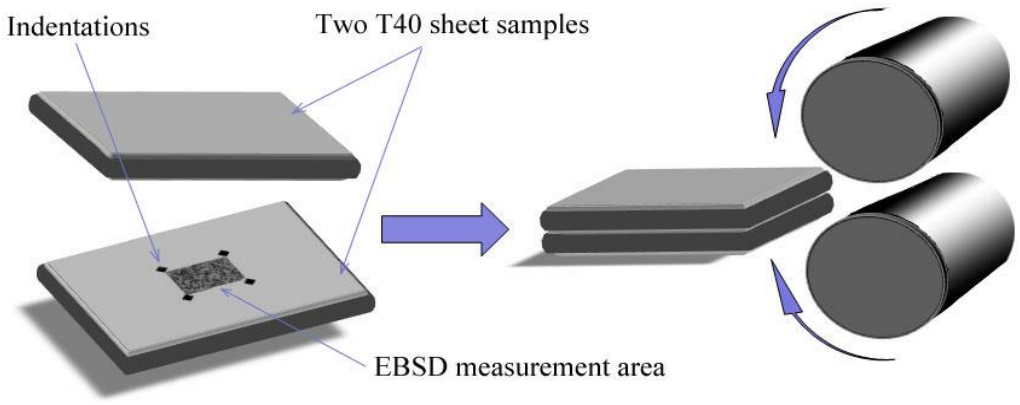

Figure 1: Schematic description of the rolling of the sample.

Crystallography and identification

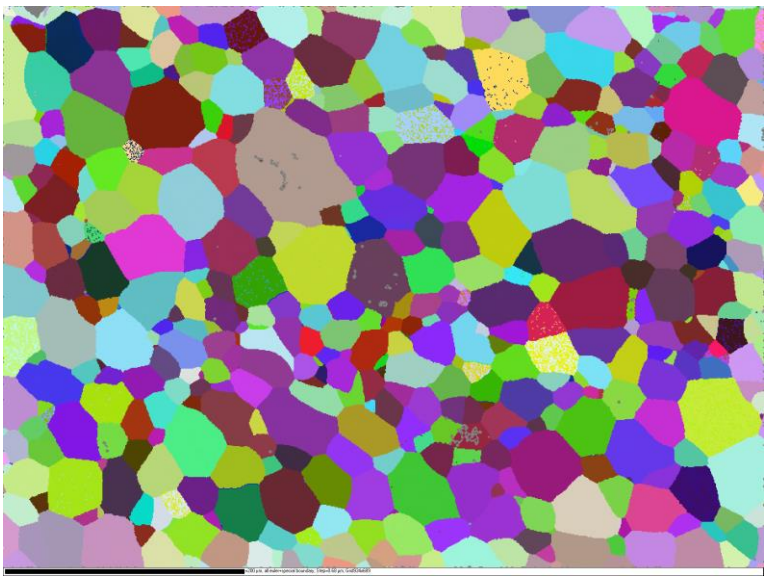

Fig 2 : EBSD map T40 after annealing (bold line scale = 200µm)

The grain size of the sample ranges from 20 to 60 µm (fig2). It is well known that such large grains favour the formation of twins during deformation. We have examined more than 50 grains in this individual follow-up and identified all the twin types, their variants and their order of appearance. We found only compressive twin ($(11\bar{2}2)$ or C Type) and tension twin ($(10\bar{1}2)$ or T1 type) (see table 2), and we did not find T2 or $(11\bar{2}1)$ tension twin. The activation of these twins depends only on the initial orientation of the grain and the local stress tensor which is a function on the applied forces. Furthermore with the increase of the deformation, secondary twins appear inside primary twins: C compression twins inside T1 tension twins or T1 tension twins inside C compression twins [6,23,27,28]. Generally these second generation of twins are called secondary or double twin.

Table 2: list of slip and twin systems in Titanium

Slip/Twin	$\vec{b}$	Slip system	Notation
Basal	<a>	$\{0002\}\langle 11\bar{2}0\rangle$	B<a>
Prismatic	<a>	$\{1\bar{1}00\}\langle 11\bar{2}0\rangle$	P<a>
Pyramidal π_1	<a>	$\{1\bar{1}01\}\langle 11\bar{2}0\rangle$	π_1<a>
Pyramidal π_1	<c+a>	$\{1\bar{1}01\}\langle 11\bar{2}\bar{3}\rangle$	π_1<c+a>
Pyramidal π_2	<c+a>	$\{1\bar{1}22\}\langle 11\bar{2}\bar{3}\rangle$	π_2<c+a>
Tension Twin	--	$\{10\bar{1}2\}\langle\bar{1}011\rangle$	T1
Tension Twin	--	$\{11\bar{2}1\}\langle\bar{1}\bar{1}26\rangle$	T2
Compression Twin	--	$\{11\bar{2}2\}\langle\bar{1}\bar{1}23\rangle$	C

To identify the type of twin system and the active variants (Table 3) that accommodate the plastic deformation, trace analysis is used (Fig 3).

Table 3: list of variant for compression (C) and tension twin (T1)

Compression C		Tension T1	
CV1	$(11\bar{2}2)\langle 11\bar{2}\bar{3}\rangle$	**T1V1**	$(10\bar{1}2)\langle\bar{1}011\rangle$
CV2	$(\bar{2}112)\langle\bar{2}11\bar{3}\rangle$	**T1V2**	$(01\bar{1}2)\langle 0\bar{1}11\rangle$
CV3	$(\bar{1}2\bar{1}2)\langle\bar{1}2\bar{1}\bar{3}\rangle$	**T1V3**	$(\bar{1}102)\langle 1\bar{1}01\rangle$
CV4	$(\bar{1}\bar{1}22)\langle 11\bar{2}\bar{3}\rangle$	**T1V4**	$(\bar{1}012)\langle 10\bar{1}1\rangle$
CV5	$(2\bar{1}\bar{1}2)\langle 2\bar{1}\bar{1}\bar{3}\rangle$	**T1V5**	$(0\bar{1}12)\langle 01\bar{1}1\rangle$
CV6	$(\bar{1}2\bar{1}2)\langle\bar{1}2\bar{1}\bar{3}\rangle$	**T1V6**	$(1\bar{1}02)\langle\bar{1}101\rangle$

Twinning is treated as a slip system to calculate the Schmid Factor (SF). Also the trace angles of all possible twin planes on the grain surface are calculated with respect to the sample

coordinate system. Then the trace angles of the observed twin planes are measured in the same coordinate system and compared with the calculated ones to identify the corresponding active twin system and twin variant. The schematic of the position of a slip line (or twin line) on the sample surface is shown in Fig 3.

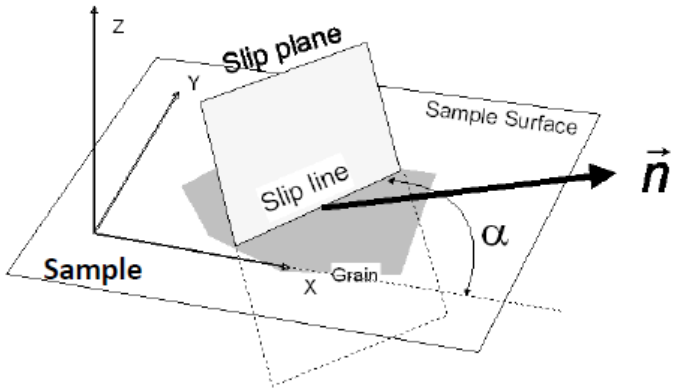

Figure 3: Slip (twin) line trace on the sample surface.

The figure 4 follows step by step the onset of primary and secondary twin. The results show that the twin variants that appear in the grain to accommodate the deformation are seldom those with the highest SF. In fact, only less than 50% of the variants with the highest SF are selected. Often in the equiaxed grains, several twin variants can appear, as shown in Fig. 4; whereas in those with elongated shape, only one variant appears, but it appears repeatedly, as shown in Fig. 5 b. This indicates that the shape of the initial grain also influences the selection of the variants.

We therefore decided to measure the length of each twin variant that appears (Fig. 6) and also calculate the maximum length of all variants that may occur to analyze the selection of the variant in terms of absorbed energy, as explained in the following.

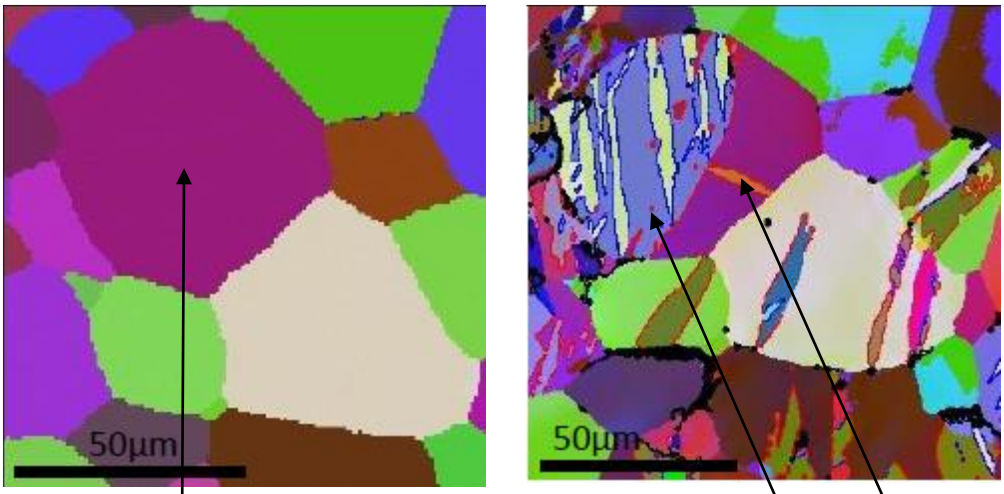

a) Initial: Orientation of the matrix :(108.7, 18.5, 28)

b) Several Variants appear in the grain. They appear one after another.(CV4 and CV2)

Inside CV4 (orientation : 78.7, 85.8, 48) we have tension twin (T1V5)

Figure 4: Micrographies of the same equiaxed grain a) initial structure, b) after 10% of rolling.

a) Orientation of the matrix :(75.2, 32.3, 15)

b) compression twin CV3

Figure 5: a) initial grain; b) with one variant after 10 % deformation

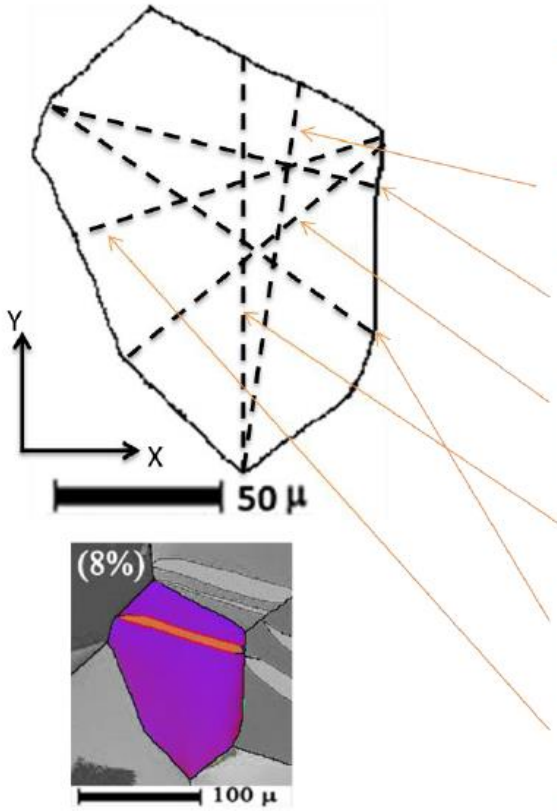

Variants	SF	Angles between twin trace and X (°)	Free path (L) (µm)
Variant $(11\bar{2}2)$	0.47	84.1	75
Variant $(\bar{1}2\bar{1}2)$	0.45	162.8	70
Variant $(\bar{2}112)$	0.34	39.3	65
Variant $(\bar{2}\bar{1}22)$	0.19	90.5	85
Variant $(1\bar{2}12)$	0.26	142.0	75
Variant $(2\bar{1}\bar{1}2)$	0.43	14.6	60

Figure 6: Sketch of a grain with orientation (x,y,z) and maximal length of the different variant.

Deformation Energy [27, 28]

The decrease of the internal energy of the material must be sufficient to deliver the energy spent by the stress/strain field to create (to propagate) the twin. To calculate this plastic deformation energy in a grain we have made some assumptions:

-The material is an ideal (i.e., no strain hardening) rigid- plastic body,

-The material obeys to the Von Mises (VM) yield criterion (here, each type of twin as its own yield stress (note σ_y) express in the sample frame),

- A grain as the same stress that the sample (Sachs assumption),

- We are in plane strain (no width => ε_{22}=0), the stress are constant in the thickness, and the axes of the sample frame are the principal axes.

So with these assumptions we found that the strain and stress tensor have the following form:

$$\bar{\bar{\epsilon}} = \begin{pmatrix} \epsilon_{11} & 0 & 0 \\ 0 & 0 & 0 \\ 0 & 0 & \epsilon_{33} \end{pmatrix} \quad (1)$$

$$\bar{\bar{\sigma}} = \begin{pmatrix} \sigma_{11} & 0 & 0 \\ 0 & \sigma_{22} & 0 \\ 0 & 0 & \sigma_{33} \end{pmatrix} \quad (2) \qquad \text{with } \sigma_{22} = \frac{1}{2}(\sigma_{11} + \sigma_{33}) \ (3)$$

In this case the VM criterion is:

$\sigma_{11} - \sigma_{33} = \frac{2}{\sqrt{3}}\,\sigma_y$ (*There is plastic flow when:* $\sigma_{33} = -\sigma_y$) (4)

The volume of the material doesn't change during the deformation, so: $\epsilon_{11} = -\epsilon_{33}$ (5)

As the material is a rigid plastic body for the twinning, we can calculate easily the plastic strain energy (by grain unit volume) by the relation above:

$$W = \epsilon_{11}\sigma_{11} + \epsilon_{33}\sigma_{33} \ (6)$$

If we introduce (5) to (6) we have: $W = -\epsilon_{33}\sigma_{11} + \epsilon_{33}\sigma_{33} = -\epsilon_{33}(\sigma_{11} - \sigma_{33})$ (7)

$$(4) \text{ to } (7) : W = -\frac{2}{\sqrt{3}}\,\sigma_y\epsilon_{33}. \ (8)$$

ϵ_{33} is the macroscopical strain. Tenckhoff[30] and Reed-Hill[29] have shown that the macroscopical strain is link to the strain produce by the twin by the volume (V) of these twin.

Here: $\epsilon_{33} = V\epsilon'_{33}$ (9) with ϵ'_{33} is the twinning deformation expressed in the sample frame

The plastic deformation comes: $W = -\frac{2}{\sqrt{3}}\,V\sigma_y\epsilon'_{33} = \frac{2}{\sqrt{3}}\,V\,W_{twin}$ (10)

$$W_{twin} = \tau\gamma|_{twin\ frame} = -\sigma_y\varepsilon'_{33}\big|_{sample\ frame} \ (11)$$

Where σ_y is the critical resolved shear stress required (=shear stress τ in twin frame expressed in sample frame) to activate the twinning system and ε'_{ij} is the corresponding twinning deformation. The twinning system will be active when the resolved shear stress reaches the corresponding critical value σ_y.

We introduce the grain size effect by expressing the critical resolved shear stress according to a Hall Petch (HP) type equation:

$$\sigma_y = \sigma_0 + \frac{k}{\sqrt{L}} \qquad (12)$$

with σ_0 and k constants, σ_0 representing the stress when the length of the grain is infinite. L is the free path of the twin before encountering an obstacle (grain boundary, precipitate or other twins). Then the deformation energy can be expressed as:

$$\begin{aligned} W &= (\sigma_0 + \frac{k}{\sqrt{L}})\varepsilon'_{33} \\ &= \sigma_0\varepsilon'_{33} + \frac{k}{\sqrt{L}}\varepsilon'_{33} \end{aligned} \qquad (13)$$

In Eq. (13), σ_0 and k are unknowns. Taking into account that twinning is activated when the size of a grain exceeds a certain value below which only crystal glide can be activated, we can deduce that the second term of the equation is dominant. Rearranging Eq. (13) we obtain:

$$\frac{W - \sigma_0\varepsilon_{33}}{k} = \frac{\varepsilon'_{33}}{\sqrt{L}} \quad (14)$$

In the right hand term of Eq. (14), ε_{33} is accessible to the calculation and L, is accessible to the experiment. In the following we will mainly focus on this term, $\frac{\varepsilon'_{33}}{\sqrt{L}}$. Clearly, the length (L) of the free path of a twin lamella in a grain can be visualized with its boundary traces on the sample observation plane. The maximum longitudinal length of the twin lamella appearing on the sample observation plane is determined as L for each twin variant, as illustrated in Fig. 5. In the present work, the $\frac{\varepsilon'_{33}}{\sqrt{L}}$ term is calculated in the sample coordinate system.

The gradient displacement tensor was first expressed in an orthonormal reference frame defined by the related twinning elements [28]. The unit vector normal to the twinning plane, the unit vector normal to the shear plane and the unit vector in the twinning direction define this reference frame. In this frame the displacement gradient tensor has a particularly simple form:

$$e_{ij} = \begin{pmatrix} 0 & 0 & s \\ 0 & 0 & 0 \\ 0 & 0 & 0 \end{pmatrix} \quad (15)$$

With $s = \frac{|\gamma^2-3|}{\gamma\sqrt{3}}$ for the (10-12) twin and $s = \frac{2(\gamma^2-2)}{3\gamma}$ for the (11-22) twin where $\gamma = {}^{c}/_{a}$ ratio of titanium[9] , the displacement gradient tensor for the two types of twins can be obtained as:

Compression (11-22) Tension (10-12)

$$\begin{pmatrix} 0 & 0 & 0.218 \\ 0 & 0 & 0 \\ 0 & 0 & 0 \end{pmatrix} \qquad \begin{pmatrix} 0 & 0 & 0.175 \\ 0 & 0 & 0 \\ 0 & 0 & 0 \end{pmatrix} \quad (16)$$

Through coordinate transformation, this displacement gradient tensor can be expressed in the crystal coordinate system (here we choose the orthonormal reference system set to the hexagonal crystal basis and the setting follows the Channel 5 convention, i.e. $e_2//a_2$ and $e_3//c$). With the Euler angles measured by SEM/EBSD that represent a set of rotations from the sample coordinate system to the orthonormal crystal basis, this tensor can be further transformed into the macroscopic sample coordinate system. If G is the coordinate transformation matrix from the macroscopic sample coordinate system to the orthonormal twin reference system, the displacement gradient tensor with respect to the sample coordinate system can be expressed as:

$$(e_{ij}^{sample\ frame}) = G \quad (e_{ij}^{crystal\ frame})G^{-1} \quad (17)$$

Thus the deformation tensor in the macroscopic sample coordinate system can be obtained as the symmetrized displacement gradient:

$$\varepsilon'_{ij} = \frac{1}{2}\left(e_{ij} + e_{ji}\right) \qquad (18)$$

With Eq. (18), the strain term can thus be calculated and the energy term $\frac{\varepsilon'_{33}}{\sqrt{L}}$ in Eq. (14) can thus be calculated too.

Results

The energy term $\frac{\varepsilon'_{33}}{\sqrt{L}}$ in Eq. (14) has been calculated for all the examined grains. We detail two cases of primary twinning, one with compression twin (C) and one with tension twin (T1), and shown in Table 4. We have found only a few (only 2) primary tension twin (fig 2d). Primary twins are compression this is because the annealing time was not sufficient to erase the rolling texture (most grain have c axes tilted 30 ° in the Transverse direction) (fig 7 a).

a) Initial Texture Pole figure {0002} RD// horitizontal axes	b) Primary C twin RD// horitizontal axes	c) Secondary T1 twin RD// horitizontal axes	d) PrimaryT1 twin RD// horitizontal axes
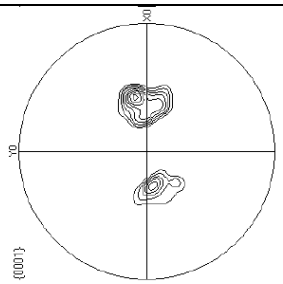	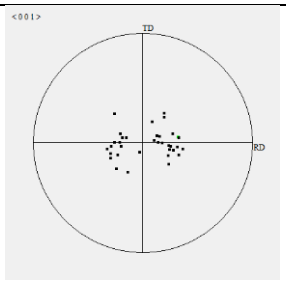	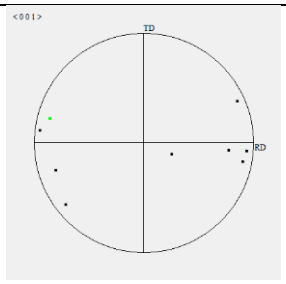	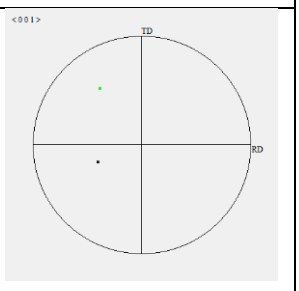

Figure 7: pole figure of a) initial texture and b to d orientation of grains who have twinned

The examples for secondary twinning are shown in Table 5. It should be noted that in a primary compression twin, only secondary tension twin can form (and vice versa). In the table, the orientation of the grain is given by the Euler angles (φ_1, ϕ, φ_2) with respect to the

macroscopic sample coordinate system are measured by EBSD/SEM. With the experimental orientation, the SF, the ε'_{33} and the $\frac{\varepsilon'_{33}}{\sqrt{L}}$ are calculated for all the twin variants (either tension or compression type). The $\frac{\varepsilon'_{33}}{\sqrt{L}}$ is calculated using the corresponding measured grain diameter. The experimentally observed active variant is highlighted in grey in all the tables . The maximum SF of the variants is in dark bold. It is seen that the activated variants are not those with the highest SF but the ones with highest absolute value of $\frac{\varepsilon'_{33}}{\sqrt{L}}$. The variant which has the highest local stress will consume the most energy to be activated. These results indicate that the SF as the variant selection criterion gives 45% to 50% correct prediction, whereas taking account of the mean free path gives 80% (and more than 95% in the case of secondary twin). When the initial grain is equiaxed, the free path of each variant can vary to a large extent, as shown in Fig. 4. In such a case, the activated variant is the one that has the lowest $\frac{\varepsilon'_{33}}{\sqrt{L}}$ (in fact, the highest absolute ratio).

Table 4: Results for primary twin

C Twin	Orientation of grain:{98.4, 36.5, 35.2}				Orientation of grain:{117.3, 36.5, 35.2}			
	SF	ε'_{33}	Length(μm)	$\varepsilon'_{33}/\sqrt{L}$	SF	ε'_{33}	Length(μm)	$\varepsilon'_{33}/\sqrt{L}$
CV1	0,027	0,0062	49,5	0,9	-0,430	-0,0939	40,9	-14,7
CV2	-0,271	-0,0592	53,4	-8,1	-0,314	-0,0685	40,8	-10,7
CV3	**-0,353**	-0,0771	57,0	-10,2	-0,095	-0,0204	45,5	-3,0
CV4	-0,346	-0,0758	51,3	**-10,6**	-0,161	-0,0349	45,5	-5,2
CV5	-0,309	-0,0674	57,0	-8,9	-0,382	-0,0835	47,0	-12,2
CV6	-0,017	-0,0034	53,8	-0,5	**-0,431**	-0,0944	40,0	**-14,9**

T1 Twin	Orientation of grain:{112.5, 133.4, 6.7}			
	SF	ε'_{33}	Length(μm)	$\varepsilon'_{33}/\sqrt{L}$
T1V1	**-0,237**	-0,041	43,0	**-6,3**
T1V2	-0,055	-0,009	34,5	-1,6
T1V3	-0,102	-0,018	38,8	-2,8
T1V4	-0,226	-0,040	47,8	-5,7
T1V5	0,028	0,005	50,3	0,7
T1V6	-0,030	-0,005	49,2	-0,8

The effect of domains is explained by Schuman et al [27] in a simpler manner. Each domain must be considered as a new grain with its own dimensions so that new variants could be activated through this size effect.

In the case of an elongated grain shape, one variant can repeatedly appear several times, as shown in Fig. 5. Although the appearance of the twin changes the dimension of the grain, the

size of the free path of this twin remains unchanged, i. e. the favorable orientation (high absolute value of the factor $\frac{\varepsilon'_{33}}{\sqrt{L}}$) of this variant remains, therefore it appears repeatedly. Generally, with the increase of the deformation, each twin lamella thickness and finally the whole grain is twinned out.

Table 5: Results for secondary twin (Primary twin is Compression Twin C, secondary twin is Tension twin T1)

C T1 twin	Orientation of grain:{85.2, 86.6, 10.1}				Orientation of grain:{64.4, 161.1, 11.7}			
	SF	ε'_{33}	Length(µm)	$\varepsilon'_{33}/\sqrt{L}$	SF	ε'_{33}	Length(µm)	$\varepsilon'_{33}/\sqrt{L}$
T1V1	0,014	-0	20	-0,6	0,011	0,002	31,5	0,3
T1V2	**0,442**	-0,08	25	-15,4	-0,38	-0,07	18,1	**-15,4**
T1V3	0,293	-0,05	13	-14,2	-0,28	-0,05	32	-8,7
T1V4	0,013	-0	14	-0,6	0,008	0,001	29,3	0,2
T1V5	0,432	-0,08	16	**-18,9**	**-0,4**	-0,07	31,6	-12,6
T1V6	0,285	-0,05	24	-10,1	-0,31	-0,05	23,1	-11,2

For a given orientation, the selection of variants always follows the $\frac{\varepsilon'_{33}}{\sqrt{L}}$ criterion. Different types of variant selection can occur in the new grain but it can always be explained by introducing the concept of domain [27].

Discussion

The above results demonstrate that the selection of twin variants is strongly dependent on the energy consumed to activate the twin (this is not an energy of nucleation, it is only a propagation energy) , the mean free path that the twin covers and the shape of the initial grain. Once a twin forms in a grain, it cuts the grain and thus inevitably changes the dimensions of this grain, subdividing the initial grain into three domains. The twin can be

regarded as a new grain with its own dimension and crystallographic orientation. Each time when a twin forms, the size of the parent grain is modified and thus the apparent stress on each possible twin variant will change according to the HP law. As a result, variants which did not have a sufficient level of stress through the SF can nevertheless be active in a newly created domain, despite the orientation of the initial grain not having changed. This explains why in equiaxed grains, several variants can appear. However, in the elongated grains, although the activation of the twin variant changes the dimension of the grain, it does not change the length of the free path of this variant. Thus this variant can form repeatedly as long as it does not create conditions more favorable for another variant. In such conditions, the twins activated can continue to grow until, in very often cases, the whole grain is twinned out.

A twin must be regarded as a new grain, which is a slightly different point of view than that of secondary twin. Generally, this new grain presents an elongated shape (at least at the early stage of its formation). Thus there will generally be, one activated variant in this existing twin. In fact, this notion strongly depends on the size of the twin, since, it was seen that when a grain is fully consumed by twinning there can be several variants thereafter.

When several twin variants, that do not cross the grain right through, form in one grain, the grain is divided into domains. A domain is thus limited by twin boundaries and grain boundaries. Each domain has its own crystallographic orientation (generally that of the matrix) and its own dimensions.

Currently, it is not possible to have an absolute prediction because interactions between neighbors (local field stresses and deformations) is not taken into account. In addition, we have a surface vision of a volume phenomenon (the comparison with experimental

measurement is only on a surface (2D) but the twins growth in the volume of the grain (in 3D)).

Conclusion

With the experimental examination, an energetic twin variant selection rule in titanium during deformation has been proposed. The prediction (postdiction) is correct in 80% ((and more than 95% in the case of secondary twin) of the cases, whereas that according to SF only in 50% .

For the time being, this rule has been verified with the (1012) and (1122) twins that are frequent in titanium and titanium alloys. The rule can be used to calculate the energy consumption for twin formation, i.e. the internal energy consumed to form a twin. The choice of a slip or twinning system is only based on an energy criterion. The system used will be that which will make it possible to lower as much as possible the internal energy of the material.

Calculations by ab-initio and EAM methods are undertaken to determine twinning energies. These calculations already led to results in the case of crystallographic slip [25].

Taking account of the grain size seems to be one of the essential keys to explain the variant selection. More precisely, it will introduce the concepts of domain, free path and that of new grain. Thus, a twin will be regarded as a – new - grain characterized by its size and crystallographic orientation.

**Acknowledgement:

This work was supported by the Federation of Research for Aeronautic and Space (Fédération de Recherche pour l'Aéronautique et l'Espace Thème Matériaux pour l'Aéronautique et l'Espace : project OPTIMIST (optimisation de la mise en forme d'alliage de titane)).

References:

[1] Kocks, U.F. and D.G. Westlake,. AIME MET SOC TRANS, 1967. **239**(7): p. 1107-1109.

[2] Yoo, M., Metallurgical and Materials Transactions A, 1981. **12**(3): p. 409-418.

[3] M. J. Philippe, M. Serghat, P. Van Houtte, C. Esling. Acta Metall. et Mater. 1995, 43, 1619.

[4] Y. B. Chun, S.H. Yu, S.L. Seliatin, S.K. Hwang, Mater. Sci. Eng. A 2005, 398, 209.

[5] D. H. Shin, I. Kim, J. Kim, Y.T Zhu, Mater. Sci. Eng. A 2002, 334, 239.

[6] L. Bao, J.S. Lecomte, C. Schuman, M.J. Philippe, X. Zhao, C. Esling Adv. Eng. Mater. 2010, 12, 1053.

[7] Crocker, A.G., Journal of Nuclear Materials, 1965. **16**(3): p. 306-326.

[8] Mahajan, S. and D.F. Williams, International Metallurgical Reviews, 1973. **18**: p. 43-61.

[9] Akhtar, A. Metallurgical and Materials Transactions A, 1975. **6**(4): p. 1105-1113.

[10] Ishiyama, S., S. Hanada, and O. Izumi, Journal of the Japan Institute of Metals, 1990. **54**(9): p. 976-984.

[11] Churchman, A.T. J. Inst. Metals, 1954. **83**: p. 39-40.

[12] Song, S.G. and G.T. Gray,. Acta Metallurgica et Materialia, 1995. **43**(6): p. 2339-2350.

[13] Goo, E. and K.T. Park, , 1989. **23**(7): p. 1053-1056.

[14] Proust, G., C.N. Tomé, and G.C. Kaschner,. Acta Materialia, 2007. **55**(6): p. 2137-2148.

[15] X. Wu, K. Kalidindi, S.R. Necker, C. Salem, Acta Mater. 2007, 55, 423.

[16] Wonsiewicz, B.C. and W.A. Backofen. Transactions of The Metallurgical Society of AIME, 1967. **239**.

[17] Partridge, P.G.. Metallurgical Reviews, 1967. **12**(118): p. 169-194.

[18] Meyers, M.A., O. Vöhringer, and V.A. Lubarda. Acta Materialia, 2001. **49**(19): p. 4025-4039.

[19] Philippe, M.J., C. Esling, and B. Hocheid. Textures and Microstructures, 1988. **7**: p. 265-301.

[20] F. Le Cras, M. serghat, J.J. Fundenberger, M.J. Philippe, C. Esling Proc. Titanium 95, 1, 659.

[21] J. J. Fundenberger, , M.J. Philippe, F. Wagner, C. Esling. Acta Mater. 1997, 45, 4041. &

[22] T.A. Mason, J.F. Bingert, G.C. Karschner, S.I. Wright, R.J. Larsen, Metall. Mater. Trans. A 2002, 33, 949.

[23] L. Bao, C. Schuman, J.S. Lecomte, M.J. Philippe, X. Zhao, L. Zuo, C. Esling. Comput, Mater, Con. 2010, 15, 113.

[24] E. Martin, L. Capolongo, L. Jiang, J.J. Jonas, Acta Mater. 2010, 58, 3970.

[25] J. J. Jonas, S. Mu, T. Al-Samman, G. Gottstein, L. Jiang, E. Martin Acta Mater. 2011, 59, 2046.

[26] A. Poty,J.M. Raulot, H.Xu, D. Rodney, J. Bai, C. Schuman, J.S. Lecomte, M.J. Philippe, C. Esling. J. Appl. Phys, vol 110 Issue 1 , 2011

[27] C. Schuman, L. Bao, J.S. Lecomte, Y. Zhang, J.M. Raulot, M.J. Philippe, C. Esling, Adv. Eng. Mat., (2011)

[28] C. Schuman, L. Bao, J.S. Lecomte, Y. Zhang, J.M. Raulot, M.J. Philippe, C. Esling, Adv. Eng. Mat., (2012)

[29] R.E. Reed-Hill, J.P. Rosi, H.C. Rogers, Deformation twinning, vol 25, (1964), Gordon and Breach science publishers

[30] E. Tenckhoff, , ASTM , special technical publication STP 966, 1988